Table 1. *Dose-dependent uptake clearance of HbV in liver, spleen, kidney, lung and heart after ^{125}I-HbV administration in mice*

All mice received a single injection of ^{125}I-HbV (1, 10, 200 and 1400 mg Hb /kg) containing 5% rHSA. The uptake clearance for each organ was calculated by integration plot analysis at designated times from 1 min to 30 min after injection.

dose (mg/kg)	CL_{uptake} (μL/hr)				
	liver	spleen	kidney	lung	heart
1	2608±654	1018±188	19±9.4	3.5±0.9	0.14±0.06
10	1473±440	786±94	18±8.1	2.5±0.2	0.38±0.09
200	452±114	102±36	25±9.2	1.3±0.2	0.06±0.02
1400	256±37	51±6.1	27±9.4	0.6±0.2	0.14±0.06

The values are mean ± S.D. (n=3-6).

そこで，初代肝実質及び肝内皮細胞，さらにはクッパー細胞の代替としてマウス単球由来マクロファージであるRAW 264.7細胞を用い，HbVの取り込みに関与する細胞腫の探索を行ったところ，初代肝実質及び肝内皮細胞において，[125]I-HbVの特異的な取り込みは認められなかったが，RAW 264.7細胞においてのみ，[125]I-HbVの特異的な取り込みと分解が認められた．また，RAW 264.7細胞における[125]I-HbVの取り込みに飽和現象がみられたことから，肝臓及び脾臓への取り込みにはクッパー細胞及び脾臓マクロファージの関与が明らかとなった．先述したように，リポソーム製剤は肝臓や脾臓などのMPSによって取り込まれ易く[20]，この過程には，補体系活性化によるリポソームのオプソニン化が関与すると考えられている．また，リポソーム製剤の取り込み経路としてはCD14, CD36, CD51/61などのスカベンジレセプターを介した経路も報告されている[21]．さらに我々は最近，補体系を不活化させた培養液中において，RAW 264.7細胞によるHbVの特異的な取り込まれることを見出しており，HbVの肝臓及び脾臓への取り込み過程には補体系活性化による経路に加えて，スカベンジレセプターなどが一部関与している可能性が示唆された．

3　HbV構成成分の体内動態解析[18]

人工酸素運搬体は赤血球代替物であるため通常の薬剤とは異なり，一度に大量投与される．そのため，一般的な薬物に比べて予期せぬ副作用や生体内蓄積性を示すことが懸念される．特にHbVの構成成分であるHbは腎傷害，高血圧の原因となり[22]，脂質膜成分（特にコレステロールの蓄積）は腎臓や心血管疾患のリスクファクターに成り得る[23]．そこで，HbVの内部Hb及び膜構成成分の一つであるコレステロールをそれぞれ[125]I及びトリチウム（[3]H）で標識したHbV（[125]I-HbV及び[3]H-HbV）を用い，臨床推奨量とされる1400 mg Hb/kgでddYマウス及びSDラットに投与し，HbV構成成分の詳細な体内動態的特性の検討を行った．

ddYマウスに[125]I-HbVあるいは[3]H-HbVを静脈内投与後の[125]I-HbV及び[3]H-HbVはほぼ同様の血漿中濃度推移を示し，濃度推移曲線より得られた体内動態パラメータもほぼ一致した．さらに原子発光分析法を用いて，Hb構成元素であるヘム鉄の血漿中濃度を併せて測定したところ，[125]I-HbV及び[3]H-HbVの推移とよく一致した．これらの結果は，HbVが血中で分解を受けることなく，小胞体構造を保持した形で血中を循環していることを強く示唆している．

また，[125]I-HbV及び[3]H-HbVともに，HbVの主要分布臓器である肝臓及び脾臓に分布していた．そこで，肝臓及び脾臓における経時的な分布推移の検討を行い，CL_{uptake}を算出したところ，[125]I-HbV及び[3]H-HbVでよく一致し（Liver; 256 ± 37, 301 ± 41: Spleen; 51 ± 6, 43 ± 12 μL/hr, for ^{125}I-HbV and ^{3}H-HbV, respectively），HbVは小胞体構造を保持した形で臓器へ取り込まれることが示唆された．しかしながら体内分布を経時的に確認したところ，投与数時間後からの[125]I-HbV及び[3]H-HbVの挙動は明らかに異なった．すなわち，[125]I-HbV投与では7日以内に放射活性が臓器中から消失したが，[3]H-HbV投与においては14日後まで活性が認められた．このことより，HbVは肝臓及び脾臓において，脂質成分とHbに分解され，それぞれの代謝，排泄経路は異なることが示唆された．

そこで[125]I-HbV及び[3]H-HbVの排泄経路について調べた結果，[125]I-HbV投与時ではその放射活性の84％ が7日以内に尿中へ排泄されたのに対して，糞中への排泄は数%であった．一方，[3]H-HbVは70％ 以上が糞中に排泄されていた．また，胆汁中にも[3]H活性が認められたため，脂質成分は分解された後，胆汁中から糞中へ排泄されることが示唆された．加えて，SDラットに[125]I-HbV及び[3]H-HbVを1400 mg Hb/kgで投与し，同様の検討を行ったところ，マウスと同様の挙動を示した．
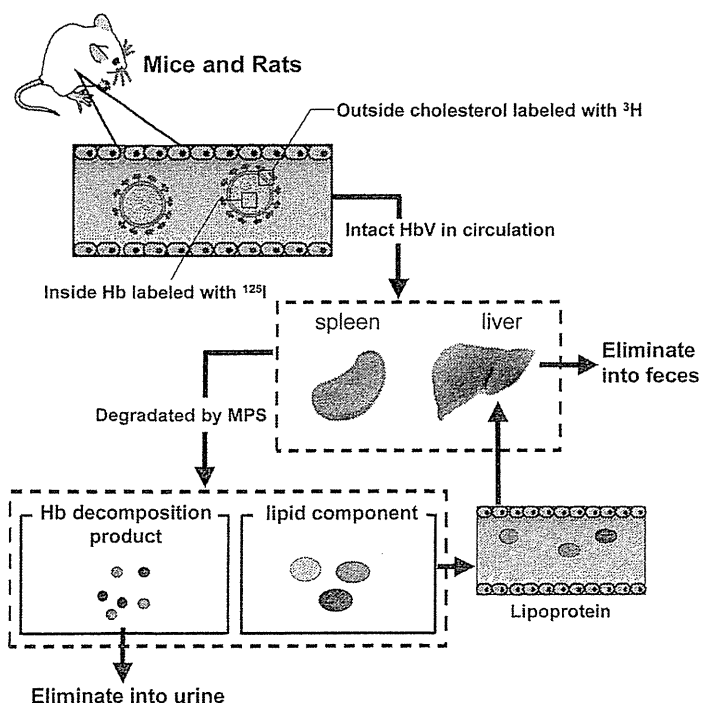

Fig. 4. Representation of a sequence of HbV disposition, metabolism and excretion from pharmacokinetic examinations using ^{125}I-HbV and ^{3}H-HbV.

これらの検討により，HbVは小胞体構造を保持した状態で血中を循環し，小胞体構造を保持したまま，主に肝臓・脾臓に存在するMPSに取り込まれ分解をうけると結論付けた．また，HbV分解後では内部Hbと脂質成分の挙動は異なり，前者は臓器においてアミノ酸レベルまで分解を受けた後に，速やかに臓器から消失し，主に尿中に排泄されるのに対して，脂質膜成分は臓器に一時的な蓄積性を示し，その大部分は胆汁中から糞中へ排泄される一連の体内動態特性が明らかとなった（Fig. 4）．これらの結果は，HbVが臨床使用量とされる1400 mg Hb/kgという大量投与された場合においても，生体蓄積性が少なく，また，内因性のHbや脂質成分と同様の経路で代謝排泄されることを示唆しており，HbVが代謝・排泄性に優れていることが強く示唆された．しかしながら，今回の標識体は内部Hbのグロビン蛋白または脂質膜構成成分のコレステロールを標識したものであるため，今後，内部Hb中のヘムや他の脂質膜構成成分（リン脂質など）の動態特性に関しても詳細な検討を行う必要があると考えられる．

4 HbVによるABC現象の誘導[24]

　HbVを現行の輸血代替として使用されることを想定した場合，同一患者へ繰り返し投与される状況は十分に想定される．近年，リポソーム製剤，特にPEG修飾リポソームにおいて，2回目に投与したPEG修飾リポソームのCLが1回目投与時と比べて著しく増大する，いわゆるABC現象が幅広く認識され[17]，リポソーム製剤を上市する際には頻回投与時における体内動態特性の変化について理解することが重要であると考えられる．そこで，PEG修飾新規リポソーム製剤であるHbVにおいても，ABC現象が誘導されるか否かについて検討した．

　マウスに非標識HbVを用いて，一般にPEG修飾リポソーム製剤でABC現象が誘導されると知られている低投与量（0.1 mg Hb/kg）及びHbVの臨床推奨量である高投与量（1400 mg Hb/kg）を静脈内投与し，初回投与7日後に再び同じ投与量の^{125}I-HbVを投与したところ，低投与量（0.1 mg Hb/kg）時では，2回目に投与した^{125}I-HbVが速やかに血漿中から消失した．この時，CLは著しく増大し，ABC現象の誘導が確認された（Fig. 5A）（CL；3.69 ± 0.4 and 22.3 ± 8.1 mL/hr, p<0.001, for the first and second injections, respectively）．一方，高投与量（1400 mg Hb/kg）時は，2回目に投与した^{125}I-HbVの血中CLの増大は確認されず，ABC現象は誘導されなかった（Fig. 5B）（CL; 0.12 ± 0.04 and 0.14 ± 0.05 mL/hr, not significantly, for the first and second injections, respectively）

　ABC現象の誘導には，クッパー細胞による取り込み量の増大が観察されることが報告されていることから[25]，肝臓への分布を投与後72時間まで追跡した．その結果，低投与量（0.1 mg Hb/kg）群の場合，初回投与時は，投与後3分で投与量の10％程度が分布したのに対し，2回目投与時では投与量の50％以上が分布していた．この変化は，CL$_{uptake}$にも有意な差として反映された（CL$_{uptake}$；3.5 ± 0.4 and 29.6 ± 18 mL/hr, p<0.01, for the first and the second injection, respectively）．

対称的に，高投与量（1400 mg Hb/kg）時では，CL$_{uptake}$のわずかな増大が確認されたものの，低投与量（0.1 mg Hb/kg）時のような有意な変化は確認されなかった（CL$_{uptake}$；0.26 ± 0.04 and 0.37 ± 0.03 mL/hr, p<0.05, for the first and the second injection, respectively）．

　これまでの報告によると，ABC現象の誘導には初回投与に呼応して脾臓から分泌されたIgM抗体が2回目投与されたPEG修飾リポソームに結合する結果，クッパー細胞に認識され易くなり，取り込み量の増加と，それに伴う血中滞留性の減少といった一連のメカニズムが提唱されている[26]．そこで，HbV
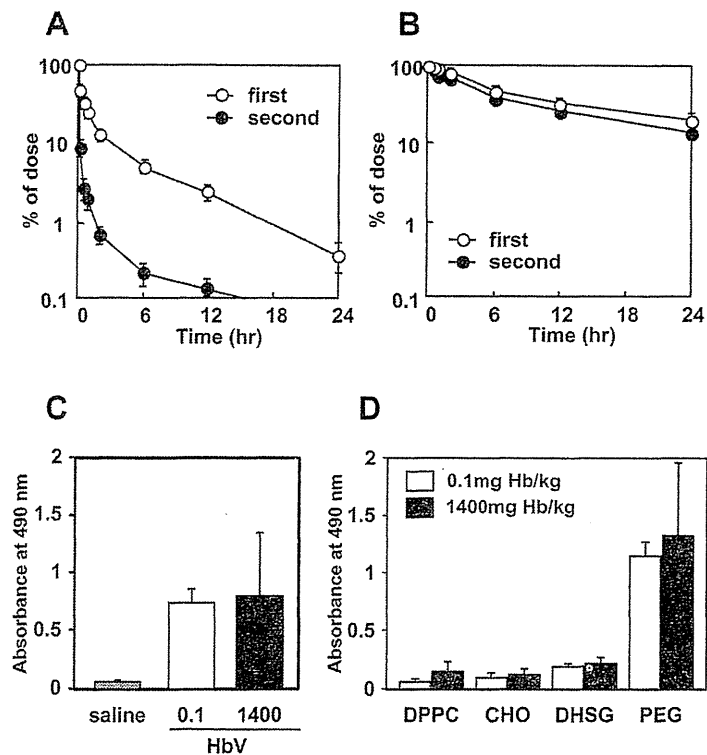

Fig. 5. Plasma concentration curve of ^{125}I-HbV after the first injection (open circle) or the second injection (closed circle) of ^{125}I-HbV to mice at a dose of 0.1 mg Hb/kg (A) or 1400 mg Hb/kg (B). Male ddY mice received a single injection of a non-labeled HbV suspension or ^{125}I-HbV to the tail vein at a dose of 0.1 or 1400 mg Hb/kg. Seven days after the first injection of the non-labeled HbV suspension, the same ddY mice received the ^{125}I-HbV suspension to the tail vein. Blood was collected from the inferior vena cava under ether anesthesia, and plasma was obtained. Each point represents the mean ± SD (n=3-6). C, Determination of IgM against HbV after a single intravenous injection of saline (gray bars), HbV at a dose of 0.1 mg Hb/kg (open bars) or 1400 mg Hb/kg (closed bars) in mice. D, Determination of the specific recognition site of IgM against HbV after a single intravenous injection of HbV at a dose of 0.1 mg Hb/kg (open bars) or 1400 mg Hb/kg (closed bars) in mice. DdY mice were injected with saline or HbV (0.1 or 1400 mg Hb/kg) to the tail vein. At 7 day after injection of saline or HbV, blood was collected from the inferior vena cava, and plasma was obtained. IgM against HbV and each lipid component were detected with ELISA. Each bar represents the mean ± SD (n=4).

低投与量（0.1 mg Hb/kg）及び高投与量（1400 mg Hb/kg）時において抗HbV IgM産生に関する検討を行ったところ，興味深いことにABC現象の誘導されなかった高投与量（1400 mg Hb/kg）時においても，抗HbV IgMの産生が確認された（Fig. 5C）．さらに，抗HbV IgMの認識部位を特定するためにHbVの脂質膜構成成分別に検討を行ったところ，1,2-distearoyl-*sn*-glycero-3-phosphatidylethanolamine-*N*-PEG（DSPE-PEG）にのみ特異的に結合することが判明した（Fig. 5D），この結果はIshidaらのPEG修飾空リポソームにおける報告とよく一致した[27]．つまり，高投与量（1400 mg Hb/kg）時において，抗HbV IgMの産生が確認されたにも関わらず，ABC現象が誘導されなかった現象は，クッパー細胞によるHbVの取り込み過程に飽和が生じたためと推察される．事実，上述したように，HbVの高投与量時には肝臓における取り込み過程に飽和が確認されている[18]．

以上の結果から，臨床想定される高投与量（1400 mg Hb/kg）条件下では，頻回投与によるABC現象は見掛け上誘導されず，薬理効果への影響は少ないものと考えられるが，安全な投与設計を確立するためには，今後，様々な病態で同様の検討を行い，データを構築していく必要がある．

5 出血性ショックモデルラットにおけるHbVの体内動態解析[28]

現在上市されているリポソーム医薬のAmphotericin B内封リポソーム製剤は健常人と病態患者によって体内動態が異なることが報告されている[15,16]．このことは，同じリポソーム製剤であるHbV投与時においても健常時と病態時（大量出血時）で体内動態特性が異なる可能性が推察される．そこで，大量出血時（40％脱血）に誘発される出血性ショックモデルラットにおいてHbVの体内動態実験を行った．

まず初めに，出血性ショックモデルラットに[125]I-HbVを1400 mg Hb/kgで投与後の血漿中濃度の変化を検討した．その結果，健常時に比べ出血性ショック時において投与初期から急激な血漿中濃度の低下が確認された（Fig. 6）．血漿中濃度推移曲線より各速度論パラメータを算出したところ，健常群と比較すると出血性ショック群では$t_{1/2}$が約2/3倍に減少し（30.6 ± 4.0 and 18.1 ± 3.7 hr, p<0.01, for normal and hemorrhagic shock, respectively），それに伴って，CLの有意な増加（0.47 ± 0.04 and 0.80 ± 0.08 mL/hr, p<0.01, for normal and hemorrhagic shock, respectively）が確認された．興味深いことに，初期血漿中濃度及び中枢コンパートメントの分布容積は両群間で同じ値を示したが，末梢コンパートメントの分布容積（V_2）は出血性ショック群で約2倍に増加した．また，中枢と末梢のコンパートメント間の移行性を示すk_{12}/k_{21}の値は健常群では約0.6であるのに対して，出血性ショック時では約1.2であり1より大きくなっていた．これらV_2やk_{12}/k_{21}値の増大より，出血性ショック時には組織への移行性が亢進していることが強く示唆された．そこで，次にHbVの各臓器（腎臓，肝臓，脾臓，肺，心臓）への経時的な分布推移について検討したところ，健常群に

比べ，出血性ショック群の方が，投与初期から臓器分布が亢進していた．これらの結果より，出血性ショック時において，HbVは臓器により多く移行することが確認された．また，出血性ショック群における[125]I-HbV投与時の糞中及び尿中排泄量の経時的な推移は，健常群と同様に主に尿中へ排泄され，糞中への排泄はほとんど確認されず，排泄量においても両群間で有意な違いが認められなかった．

これらの結果から，出血性ショック時にはHbVの血中滞留性が短縮し，臨床有用性の低下が懸念されたが，このHbVの血中滞留性の短縮は，血中から臓器への移行性増大に伴う血漿中濃度の低下によるものと推察された．つまり，出血性ショック時においては，臓器中へのHbVの移行性が増大することにより，臓器中の低酸素状態を改善している可能性が示唆された．

ところで，大量出血の患者に対しては，目標Hb値まで上昇させるために濃厚赤血球製剤の頻回投与（約1時間間隔）を行っているため，HbVが現行の輸血代替として機能することを想定した場合，同一患者への頻回投与が十分に想定される．上述したようにリポソーム製剤の頻回投与にはABC現象の誘導が懸念される．そこで次に，出血性ショックモデルラットを用いてHbVを連続投与した場合の体内動態を検討した．

出血性ショックモデルラットに非標識HbVを1400 mg Hb/kgで投与し，1時間後に再び同量の[125]I-HbV（1400 mg Hb/kg）を投与した．その結果，出血性ショックモデルラットへ単回投与した時に比べ2回目投与した時の方が明らかな血中滞留性の向上が確認された（Fig. 6）．また，各速度論パラメータを算出したところ，出血性ショックモデルラットへ単回投与した時には2回目投与した時より，$t_{1/2}$は約2倍に増加した（18.1 ± 3.7 and 32.4 ± 1.1 hr, p<0.01, for one-injection group and two-injection group, respectively）．興味深いことに，この出血性ショックモデルラットへ2回目投与した際の血漿中濃度推移と
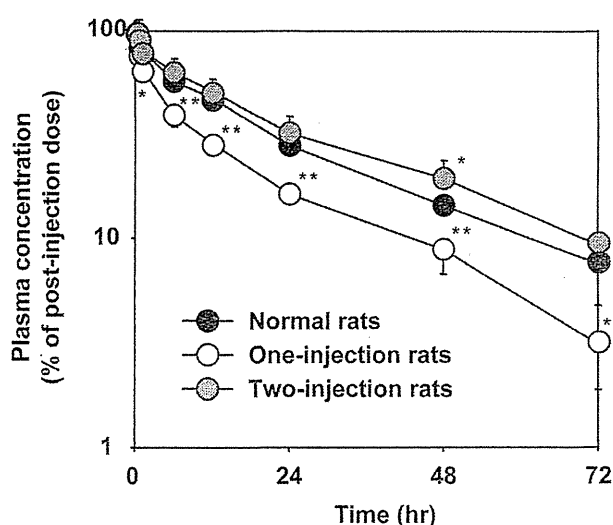

Fig. 6. Relative plasma concentration of ^{125}I-HbV after administration of 1400 mg Hb/kg via injection of normal, one-injection group or two-injection rats. Each point represents the mean ± SD (n=5). *< 0.05 or **<0.01 vs. normal rats.

速度論パラメータは，健常ラット群の結果とよく類似していた．そこでこのことを確かめるために，出血性ショックモデルラットに単回及び2回目投与時における各臓器（腎臓，肝臓，脾臓，肺，心臓）への経時的な分布推移を検討した．その結果，単回投与時に比べ，2回目投与時では投与後12時間まで臓器分布の減少が確認されたが，12時間を過ぎると，2回目投与した時の臓器分布が亢進していた．また，尿中及び糞中への排泄挙動を検討したところ，単回及び2回目投与した時では，^{125}I-HbVの排泄経路に変化は確認されなかったが，半減期の延長に伴い，2回目投与した時において排泄の遅延が観察された．加えて，出血性ショックモデルラットに非標識HbVを1400 mg Hb/kgで投与し，1時間後における抗HbV IgMの産生を調べたところ，その存在は観察されなかった．

従って，出血性ショック時に現行の濃厚赤血球と同様にHbVを1時間間隔で連続投与しても，抗HbV IgMは産生されず，ABC現象は誘導されないことが確認された．興味深いことに，出血性ショック時の初回投与時に観察された血中滞留性の低下は2回目投与時には回復しており，また，初回投与時に比べて，2回目投与時では臓器へ持続的に分布し，排泄は遅延していた．このことから，出血性ショック時にHbVを2回目投与すると，初回投与によるMPSによる取り込みの飽和により，HbVは血中に長時間滞留することで，臓器への酸素供給を持続的に行う可能性が示唆された．

6 アニマルスケールアップ[28]

HbVの臨床試験を想定した際，ヒトにおけるHbVの半減期の予測，いわゆるアニマルスケールアップは，投与設計を行う上で非常に有用である．そこで，上述したマウス・ラットの結果とSouらによる^{99m}Tc-HMPAO内封HbVを用いたウサギにおけるHbVの体内動態結果[29]を用いて，アロメトリック式（P = α・W^βP; pharmacokinetic parameters, W; body weight, α; coefficient, β; exponent）を作成し，ヒトにHbVを1400 mgHb/kgで投与した場合のHbVの半減期の予測を試みた（Fig. 7）．

その結果，ヒトにおける半減期は約96時間であると予測された．他のリポソーム製剤であるドキソルビシン封入リポソームの場合，ラットにおける半減期は35時間であるのに対して，ヒトにおいては56-90時間であった．また，経験的にリポソームのヒトにおける半減期はラットの約2-3倍であると言われており，今回の我々の結果ともよく対応していた[30]．従って，今回の検討と過去の報告を総合的に解釈すると，ヒトにおけるHbVの半減期は約3-4日ではないかと予測される．

おわりに

冒頭で述べたように，古くから前臨床試験段階における薬物動態試験の重要性が言われている．これは，薬物動態試験が，ただ単なる薬物のADMEを把握するだけでなく，薬効や副作用を予測するのに役立つからである．2008年，JAMA誌に報告された，非細胞型HBOCs投与群の死亡率および心筋梗塞発
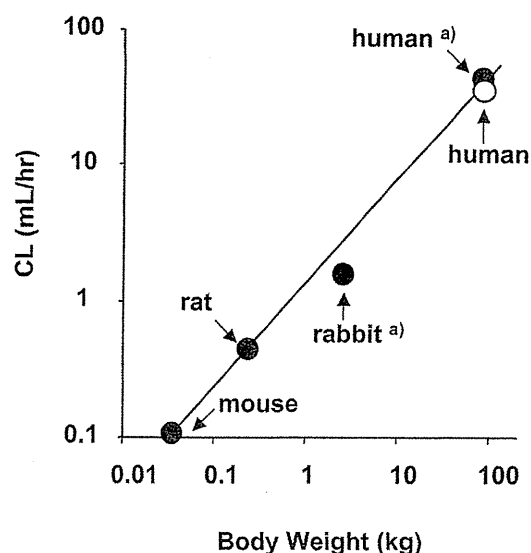

Fig. 7. Allometric relationships between body weight and body weight and clearance (CL). The linear regression of the logarithmic values was calculated using the least-squares method (y=1.466x$^{0.764}$, r^2=0.984). The extrapolated human values based on a body weight of 70 kg (open circle) are also shown. [a]Data from reference for Rabbit, and we calculated the human CL using k_e, which is from Sou et al.[11], and our estimated V_1.

症率が対照群に比べ高いことや[12]，PFCが，1年以上にわたる臓器蓄積（特に肺）により副作用が確認されたことは[14]，体内動態試験を初め，その他の試験から総合的に判断することで十分に予想できたのではないかと感じる．これらの教訓を生かし，薬物動態試験を含め，様々な前臨床試験結果を基に，HbVの安全性及び有効性を総合的に判断し，日本だけで開発が進められている細胞型HBOCsの一つであるHbVの臨床使用に向けた最終試験を進めていく必要性があるだろう．

参考文献

1. Keipert PE. Use of Oxygent, a perfluorochemical-based oxygen carrier, as an alternative to intraoperative blood transfusion. Artif Cells Blood Substit Immobil Biotechnol 1995; 23: 381-394.

2. Winslow RM. Targeted O$_2$ delivery by low-P$_{50}$ hemoglobin: a new basis for hemoglobin-based oxygen carriers. Artif Cells Blood Substit Immobil Biotechnol 2005; 33: 1-12.

3. Teramura Y, Kanazawa H, Sakai H, Takeoka S, Tsuchida E, Prolonged oxygen-carrying ability of hemoglobin vesicles by coencapsulation of catalase in vivo. Bioconjug Chem 2003; 14: 1171-1176.

4. Sakai H, Cabrales P, Tsai AG, Tsuchida E, Intaglietta M, Oxygen release from low and normal P$_{50}$ Hb vesicles in transiently occluded arterioles of the hamster window model. Am J Physiol Heart Circ Physiol 2005; 288: H2897-2903.

5. Sakai H, Takeoka S, Park SI, Kose T, Nishide H, Izumi Y,

Yoshizu A, Kobayashi K, Tsuchida E, Surface modification of hemoglobin vesicles with poly (ethylene glycol) and effects on aggregation, viscosity, and blood flow during 90% exchange transfusion in anesthetized rats. Bioconjug Chem 1997; 8: 23-30.

6. Sakai H, Tomiyama KI, Sou K, Takeoka S, Tsuchida E, Poly (ethylene glycol)-conjugation and deoxygenation enable long-term preservation of hemoglobin-vesicles as oxygen carriers in a liquid state. Bioconjug Chem 1 2000; 1: 425-432.

7. Abe H, Ikebuchi K, Hirayama J, Fujihara M, Takeoka S, Sakai H, Tsuchida E, Ikeda, H. Virus inactivation in hemoglobin solution by heat treatment. Artif Cells Blood Substit Immobil Biotechnol 2001; 29: 381-388.

8. Huang Y, Takeoka S, Sakai H, Abe H, Hirayama J, Ikebuchi K, Ikeda H, Tsuchida E. Complete deoxygenation from a hemoglobin solution by an electrochemical method and heat treatment for virus inactivation. Biotechnol Prog 2002; 18: 101-107.

9. Izumi Y, Sakai H, Kose T, Hamada K, Takeoka S, Yoshizu A, Horinouchi H, Kato R, Nishide H, Tsuchida E, Kobayashi K. Evaluation of the capabilities of a hemoglobin vesicle as an artificial oxygen carrier in a rat exchange transfusion model. ASAIO J 1997; 43: 289-297.

10. Sakai H, Masada Y, Horinouchi H, Yamamoto M, Ikeda E, Takeoka S, Kobayashi K, Tsuchida E. Hemoglobin-vesicles suspended in recombinant human serum albumin for resuscitation from hemorrhagic shock in anesthetized rats. Crit Care Med 2004; 32: 539-545.

11. Sakai H, Seishi Y, Obata Y, Takeoka S, Horinouichi H, Tsuchida E, Kobayashi K, Fluid resuscitation with artificial oxygen carriers in hemorrhaged rats: profiles of hemoglobin-vesicle degradation and hematopoiesis for 14 days. Shock 2009; 31: 192-200.

12. Natanson C, Kern SJ, Lurie P, Banks SM, Wolfe SM, Cell-free hemoglobin-based blood substitutes and risk of myocardial infarction and death: a meta-analysis. JAMA 2008; 299: 2304-2312.

13. Kennedy, T. Managing the drug discovery/development interface. Drug Discovery Today 1997; 2: 436-444.

14. Nose Y, Is there a role for blood substitutes in civilian medicine: a drug for emergency shock cases? Artif Organs 2004; 28: 807-812.

15. Walsh TJ, Yeldandi V, McEvoy M, Gonzalez C, Chanock S, Freifeld A, Seibel NI, Whitcomb PO, Jarosinski P, Boswell G, Bekersky I, Alak A, Buell D, Barret J, Wilson W. Safety, tolerance, and pharmacokinetics of a small unilamellar liposomal formulation of amphotericin B (AmBisome) in neutropenic patients. Antimicrob Agents Chemother 1998; 42: 2391-2398.

16. Bekersky I, Fielding RM, Dressler DE, Kline S, Buell DN, Walsh TJ. Pharmacokinetics, excretion, and mass balance of ^{14}C after administration of ^{14}C-cholesterol-labeled AmBisome to healthy volunteers. J Clin Pharmacol 2001; 41: 963-971.

17. Ishida T, Harada M, Wang XY, Ichihara M, Irimura K, Kiwada H. Accelerated blood clearance of PEGylated liposomes following preceding liposome injection: effects of lipid dose and PEG surface-density and chain length of the first-dose liposomes. J Control Release 2005; 105: 305-317.

18. Taguchi K, Urata Y, Anraku M, Maruyama T, Watanabe H, Sakai H, Horinouchi H, Kobayashi K, Tsuchida E, Kai T, Otagiri M, Pharmacokinetic study of enclosed hemoglobin and outer lipid component after the administration of hemoglobin vesicles as an artificial oxygen carrier. Drug Metab Dispos 2009; 37: 1456-1463.

19. Kristiansen M, Graversen JH, Jacobsen C, Sonne O, Hoffman HJ, Law SK, Moestrup SK. Identification of the haemoglobin scavenger receptor. Nature 2001; 409: 198-201.

20. Kiwada H, Matsuo H, Harashima H. Identification of proteins mediating clearance of liposomes using a liver perfusion system. Adv Drug Deliv Rev 1998; 32: 61-79.

21. Shibuya-Fujiwara N, Hirayama F, Ogata Y, Ikeda H, Ikebuchi, K.Phagocytosis in vitro of polyethylene glycol-modified liposome-encapsulated hemoglobin by human peripheral blood monocytes plus macrophages through scavenger receptors. Life Sci 2001; 70: 291-300.

22. Balla J, Vercellotti GM, Jeney V, Yachie A, Varga Z, Eaton JW Balla, G. Heme, heme oxygenase and ferritin in vascular endothelial cell injury. Mol Nutr Food Res 2005; 49: 1030-1043.

23. Groneand EF, Grone HJ. Does hyperlipidemia injure the kidney? Nat Clin Pract Nephrol 2008; 4: 424-425.

24. Taguchi K, Urata Y, Anraku M, Watanabe H, Kadowaki D, Sakai H, Horinouchi H, Kobayashi K, Tsuchida E, Maruyama T, Otagiri, M. Hemoglobin vesicles, PEGylated liposomes developed as a red blood substitute, do not induce the accelerated blood clearance phenomenon in mice. Drug Metab Dispos 2009; 37: 2197-2203.

25. Ishida T, Ichikawa T, Ichihara M, Sadzuka Y, Kiwada H, Effect of the physicochemical properties of initially injected liposomes on the clearance of subsequently injected PEGylated liposomes in mice. J Control Release. 2004; 95: 403-412.

26. Ishida T, Kiwada H. [Accelerated blood clearance (ABC) phenomenon induced by administration of PEGylated liposome]. Yakugaku Zasshi 2008; 128: 233-243.

27. Ishida T, Ichihara M, Wang X, Yamamoto K, Kimura J,

Majima E, Kiwada H. Injection of PEGylated liposomes in rats elicits PEG-specific IgM, which is responsible for rapid elimination of a second dose of PEGylated liposomes. J Control Release 2006; 112: 15-25.

28. Taguchi K, Maruyama T, Iwao Y, Sakai H, Kobayashi K, Horinouchi H, Tsuchida E, Kai T, Otagiri M, Pharmacokinetics of single and repeated injection of hemoglobin-vesicles in hemorrhagic shock rat model. J Control Release 2009; 136: 232-239.

29. Sou K, Klipper R, Goins B, Tsuchida E, Phillips WT. Circulation kinetics and organ distribution of Hb-vesicles developed as a red blood cell substitute. J Pharmacol Exp Ther 2005; 312: 702-709.

30. Gabizon A, Shmeeda H, Barenholz Y. Pharmacokinetics of pegylated liposomal Doxorubicin: review of animal and human studies. Clin Pharmacokinet 2003; 42: 419-436.

代用血漿剤

HES

Hydroxyethyl Starch

川崎医科大学名誉教授／東宝塚さとう病院名誉院長

高折益彦 著

目　　次

Determination of electrolyte concentrations in serum containing cellular artificial oxygen carrier (HbV)

Seiji Miyake [1], Jiro Takemura [1], Masuhiko Takaori [2]

Abstract

We attempted to measure electrolyte (Na, K, C) ion concentrations in serum containing an artificial oxygen carrier, HbV (hemoglobin encapsulated liposme vesicle emulsified in physiological saline), by dry chemical method using Vitros250™ (Ortho Clinical Diagnostics) or conventional wet method using TBA200FRNEO™ (Toshiba Medical System). Clinically satisfactory values of the electrolyte ion concentrations were obtained in the serum which contained the HbV at $1/2 \sim 1/32$ volume ratio and even in original HbV emulsion by the dry chemistry method. By the wet method, however, satisfactory values with clinically acceptable accuracy were not obtained when mixing volume rate of the HbV remained above 1/8 mixing rate. Subsequently the satisfactory values were obtained when mixing rate of the HbV in serum reduced less than 1/16. Reason for the above limited capacity for the wet method remained obscure. Further a trace amount of potassium ion in the HbV emulsion was a puzzle.

1. Introduction

It has been desired to develop a therapeutic agent which can restore the circulating blood volume and also oxygen carrying capacity of blood for treatment of massive hemorrhage instead of transfusion of blood, which should be stored at 5 ± 1 ℃ and compatibility test must be required. Such therapeutic agent is expected most useful for initial treatment e.g. in accident field by Medicares and most effective for life saving for out-of-hospital patient care. Up date, two types of candidate, namely hemoglobin based oxygen carrier (HBOC) and perfluorocarbon based oxygen carrier, were tested for this purpose. Unfortunately development for the latter was discontinued due to short life span in the circulation and also to thrombocytopenia after infusion[1]. On the other hand for the former, acellular type, it has been pointed out arteriolar vasoconstriction due to its scavenging effect of nitric oxide from endothelial cells[2,3,4] and consequent coronary events[5] after its infusion. Thus two pharmaceutical companies have withdrawn from the HBOC development in early 2009. Only liposome encapsulated hemoglobin vesicle which is emulsified in the physiological saline (HbV) remains to be developed further as HBOC without noticeable adverse effects.

In general, however, it has been reported that HBOCs could interfere clinical laboratory tests[6,7,8], particularly spectrophotometry used that would be interfered by absorbancy of hemoglobin molecule. Moreover laboratory test without spectrophotometry, such as polarographic examination, would be suspected to be interfered by the HbV. Since the HbV vesicles covered with non-electroconductive phospholipid, their adherence on electrode surface might effect on boundary potential.

This study was carried out to demonstrate whether or not analyzers commonly used in practice could work well for measurement of electrolyte concentrations in serum containing a cellular artificial oxygen carrier, HbV.

2. Materials and Methods

Experimental procedures were performed in Osaka Prefecture Saiseikai Noe Hospital. Blood of 18 ml was donated by six healthy, adult volunteers for each who had consented to an informed consent which had stated purpose and procedure of the study and which had been authorized by ethics committee of the hospital. The experimental procedures were examined and regulated by the ethics committee. The HbV was produced and supplied by Nippro Co (Kusatsu, Shiga), which is one of member in research group of Japanese Ministry of Health, Welfare and Labor Research Project "Clinical Applications of Artificial Oxygen Carrier H18-Drug Innovation H18-General-022". Physicochemical properties for the HbV was listed in Table 1. Medium of the HbV was collected by ultracentrifugation (50,000 G for 30 minutes) and supplied by Dr. Sakai, H. , Associate Professor, Waseda University who is also one of member in the above research project.

Table 1. Physicochemical properties of HbV

diameter of vesicle (nm)	270
vesicle volume (HbVcrit %)..................	> 30
hemoglobin content (g/dL)...................	9.7
phospholipid content (g/dL)	6.7
hemoglobin / phospholipid ratio............	1.5
carbon monooxide hemoglobin (%)	0.1
endotoxin (EU/ml)	< 0.3
sterility test	passed

Blood of 2 ml was collected in EDTA-2K tube and used to determine hematocrit and hemoglobin value. Serum of approximately 9 ml was collected in a serum separating vacuum tube by centrifugation with 1,300 G for 30 minutes from remained blood. Human albumin powder (A3782-1G Sigma-Aldrich, St Louis, Mo, U.S.A.) was dissolved at 4 % in the HbV and the medium separated from HbV.

The HbV was mixed with the original serum at 1:1 volume ratio (1/2 mixture of the HbV). Subsequently a part of this mixture was mixed with the original serum at 1:1 volume ratio and 1/4 mixture of the HbV was prepared. Then serial mixtures, 1/8 ~ 1/32, were prepared in the same manner. Electrolyte concentrations (Na$^+$, K$^+$, Cl$^-$) were measured duplicated for the original serum, serial mixtures of HbV and serum, HbV and medium of HbV with dry (D) method※ mounted on Vitros250™ (Ortho Clinical Diagnostics, Rochester, N.Y., U.S.A) and wet (W) method※ mounted on TBA200FRNEO™ (Toshiba Medical System, Ohtawara, Tochigi), respectively. The above experimental procedure was repeated on five other days. Consequently total 12 measurements were performed for each same categorized sample with the both methods, respectively. Concentration of the electrolytes in the mixtures of HbV and serum was estimated by simple, mathematical dilution equation. For example, Na$^+$ concentration in the 1/2 mixture was calculated as follows

$$\text{Na} \, (1/2 \text{ mixture}) = (1/2 \, A + 1/2 \times 0.7 \times 154) \div (1/2 + 1/2 \times 0.7)$$

where A is concentration of Na$^+$ in the original serum and 0.7 is ratio of water volume contained in aliquot volume of the HbV. Since liposome encapsulated hemoglobin vesicles were emulsified in the physiological saline at volume of 30 % , Na$^+$ concentration for the medium of HbV was adapted to Na$^+$ concentration of the physiological saline of 154 mEq/L. Mean and standard deviations for actually measured value (Am ± SD), estimated value (Em ± SD) calculated the above equation and difference (Dm ± SD) between the actually measured value and the estimated value were provided for each measurement.

When the Dm was less than 2.0 mEq/L for Na$^+$, less than 0.05 mEq/L for K$^+$ and less than 2.0 mEq/L for Cl$^-$, actually measured value corresponded to those Dms for each was evaluated as acceptably determined value, respectively.

Hematocrit and hemoglobin value for the original blood was measured with RBC pulse height detection method and sodium lauryl sulfate hemoglobin method, respectively, using Automated Hematology Analyzer XE-2100™ (Sysmex Corp. Kobe, Hyogo).

※ When we measure concentration of electrolytes in sample (serum of plasma) using the dry method which is mounted of Victors250™ (Orho Clinical Diagnostics), we inject the sample and reference solution into a small cylinder with maximum capacity of 500μl for each and put those cylinders on each proper position inside of the analyzer. The analyzer sucks up the sample and reference solution with a needle simultaneously and drops them at each proper spot on a piece of film which specific electrode for Na, K, and Cl ion are built in, respectively. After measurement we take out the film and the cylinders and discard them. Therefore any fluid remains inside of the analyzer and so we call the above procedure as dry method.

On the other hand for the wet method, each specific electrode adapted to the ions is provided in capillary part inside of an analyzer, for example, TBA200FRNED™ (Toshiba Medical System). The capillary is always filled with special reference solution for the ions and calibrated. Therefore we call it as wet method.

Table 2. Electrolyte concentrations for the original serum (serum), serial mixtures of the original HbV and the serum, and the original HbV (HbV)

			HbV	HbV in the mixtures					serum
				1/2	1/4	1/8	1/16	1/32	
Na⁺	D	Am	155.0 ± 2.2	148.0 ± 1.9	147.1 ± 2.2	146.4 ± 2.4	145.8 ± 2.6	145.3 ± 2.8	143.0 ± 2.5
		Em		148.1 ± 1.5	145.9 ± 2.1	146.4 ± 2.3	144.3 ± 2.5	144.2 ± 2.5	
		Dm		0.0 ± 0.9	1.2 ± 0.5	0.0 ± 0.5	1.5 ± 0.9	1.2 ± 0.7	
	W	Am	110.2 ± 1.4	125.7 ± 1.0	134.6 ± 1.3	138.7 ± 1.5	140.8 ± 1.7	141.8 ± 1.6	142.0 ± 1.3
		Em		147.0 ± 0.8	144.5 ± 1.0	144.8 ± 1.2	142.7 ± 1.2	142.4 ± 1.3	
		Dm		-21.3 ± 0.9	-9.9 ± 1.0	-6.1 ± 0.9	-1.8 ± 1.0	-0.5 ± 0.8	
K⁺	D	Am	ND	2.22 ± 0.18	3.12 ± 0.22	3.53 ± 0.25	3.71 ± 0.25	3.82 ± 0.25	3.93 ± 0.30
		Em		2.32 ± 0.18	3.20 ± 0.30	3.61 ± 0.29	3.77 ± 0.30	3.86 ± 0.31	
		Dm		-0.10 ± 0.06	-0.05 ± 0.07	-0.07 ± 0.07	-0.05 ± 0.08	-0.05 ± 0.08	
	W	Am	0.35 ± 0.01	1.94 ± 0.13	2.89 ± 0.17	3.36 ± 0.18	3.60 ± 0.20	3.72 ± 0.20	3.85 ± 0.25
		Em		2.27 ± 0.16	3.11 ± 0.20	3.54 ± 0.24	3.70 ± 0.25	3.78 ± 0.26	
		Dm		-0.33 ± 0.07	-0.22 ± 0.07	-0.18 ± 0.08	-0.10 ± 0.07	-0.05 ± 0.08	
Cl⁻	D	Am	150.0 ± 6.7	126.7 ± 3.5	115.9 ± 2.4	111.1 ± 2.3	109.4 ± 2.5	108.4 ± 2.1	107.0 ± 1.7
		Em		126.5 ± 1.0	116.2 ± 1.4	112.7 ± 1.7	109.1 ± 1.8	108.1 ± 1.8	
		Dm		0.2 ± 2.7	-0.3 ± 1.3	-1.6 ± 0.8	0.4 ± 1.2	0.3 ± 1.0	
	W	Am	105.3 ± 1.21	104.5 ± 0.9	104.8 ± 1.1	104.8 ± 1.3	104.9 ± 1.6	104.8 ± 1.5	103.9 ± 1.7
		Em		124.6 ± 1.1	113.6 ± 1.4	109.7 ± 1.6	106.0 ± 1.7	104.9 ± 1.7	
		Dm		-20.1 ± 0.4	-8.8 ± 0.5	-4.9 ± 0.5	-1.1 ± 0.7	-0.2 ± 0.6	

D : dry method   W : wet method   mEq/L
serum = the original serum obtained from the volunters
n = 12   mean ± standard deviations   ND : not detectable
Am : mean for acutually measured values   Em : mean for estimated values by the mixing equation (* see text)
Dm : mean for differences between Am and Em corresponded

3. Results

As shown on upper column in Table 2, Na⁺ concentration was determined as 155.0 ± 2.2 mEq/L for the original HbV and 143.0 ± 2.5 mEq/L for the original serum with the D method. Difference (Dm) between actually measured 148,0 ± 1.9 mEq/L for the 1/2 mixture and 148.1 ± 1.5 mEq/L for its estimated value was 0.0 ± 0.9 mEq/L. Subsequently Dms with the D method measurement were distributed in a range of 0.0 ± 0.5 ～ 1.5 ± 0.9 mEq/L for the 1/4 ～ 1/32 mixtures.

On the other hand with the W method, Na⁺ concentration for HbV and 1/2 mixture were measured as 110.2 ± 1.0 mEq/L and 125.7 ± 1.0 mEq/L with Dm of -21.3 ± 0.9 mEq/L , respectively. Subsequent Dm for the 1/4 and 1/8 mixture were -9.9 ± 1.0 and -6.1 ± 0.9 mEq/L, respectively and therefore those Ams were not evaluated as the acceptably determined value. Dm with Na⁺ concentration for the 1/16 and 1/32 mixture, however, was 1.8 ± 1.0 and 0.5 ± 0.8 mEq/L, respectively. Those were less than 2.0 mEq/L and those actually measured values were evaluated as the acceptably determined value.

K⁺ concentrations were listed on middle column in Table 2. K⁺ concentration for the HbV could not measured by the D method. Since the analyzer the D method mounted showed "ND" (not detectable) on its display panel. However subsequent actually measured values of K⁺ concentration for the 1/2 ～ 1/32 mixture distributed in a range of 3.12 ～ 3.82 mEq/L and Dms were less than -1.00 ± 0.06 mEq/L with the D method.

With the W method, on the other hand, K⁺ concentration for the HbV was determined as 0.35 ± 0.01 mEq/L and Dms for the serial mixtures of 1/2 ～ 1/32 distributed in a range of -0.33 ± 0.07 ～ -0.05 ± 0.08 mEq/L . Those Dms became smaller corresponded to decreasing in the mixing rate of the HbV down to the 1/32 mixture.

As shown on lower column, Cl⁻ concentration measured with the D method was 126.7 ± 3.5 mEq/L with Dm of 0.2 ±

2.7 mEq/L for the 1/2 mixture and 115.9 ± 2.4 mEq/L with Dm of −0.3 ± 1.3 mEq/L for the 1/4 mixture. With the D method, maximum Dm of −1.6 ± 0.8 mEq/L was noted in the 1/8 mixture and the other Dms did not exceed it.

Contrary with the W method, Cl⁻ concentration was measured as 105.3 ± 1.2 mEq/L for the HbV. And also Cl⁻ concentration was measured as 104.5 ± 0.9 mEq/L for the 1/2 mixture and 104.8 ± 1.1 mEq/L for the 1/4 mixture. These values differed −20.1 ± 0.4 and −8.8 ± 0.5 mEq/L from those each estimated value, respectively. However actually measured Cl⁻ concentration of 104.9 ± 1.6 for the 1/16 mixture and 104.8 ± 1.5 mEq/L for the 1/32 differed −1.1 ± 0.7 and −0.2 ± 0.6 mEq/L from each corresponded estimated value, respectively. Therefore those actually measured values were evaluated as the acceptably determined value.

As shown in Table 3, Na⁺ concentration for medium separated form the HbV was determined as 154.5 ± 2.1 mEq/L with the D method and as 151.5 ± 0.8 mEq/L with the W method. Cl⁻ concentration was determined as 156.2 ± 6.9 mEq/L for the medium with the D method and 151.3 ± 0.8 mEq/L with the W method. K⁺ in the medium was not detected with the D method but was determined as 0.40 ± 0.02 mEq/L with the W method.

Hematocrit and hemoglobin value for blood donated by the volunteers was 43.4 ± 3.7 % and 15.1 ± 1.5 g/dl, respectively.

Table 3. Electrolyte Concentrations in Medium of HbV

	Na^+	K	Cl
dry method	154.5 ± 2.1	ND	156.2 ± 6.9
wet method	151.5 ± 0.8	0.40 ± 0.02	151.3 ± 0.8

mean ± standard deviations   mEq/L
ND : not detectable

4. Discussion

Several reports have pointed out that contamination of HBOCs in blood specimen interferes clinical laboratory examinations[6,7,8], particularly spectrophotometry used. Further Miyake et al[9] have reported that exact determination of blood type, such as A, B, O, and AB, with an automated blood type analyzer could not be guaranteed until the HbV contamination would become less than 5 %. In addition it has been reported by Ali et al that contamination of HBOC in the circulating blood does interfere with pulse oxymetry for oxygen saturation monitoring.[10]. Murata et al[11], therefore, eliminated the HbV vesicles from patients' plasma by ultracentrifugation for a number of clinically laboratory tests.

Alternatively Takaori et al[12], Murata et al[13], Sou et al[14] mixed the blood with high molecular weight dextran, such as 200 ~ 600 kD, and separated the HbV vesicles entrapped into aggregated red cells and obtained HbV free plasma. These procedures separating the HbV vesicles, however, would not be applicable for clinical laboratory practice, particularly in emergency medicine. Cameron et al[15] has reported, nevertheless, that electrolyte concentrations in blood containing Hemospan™ (HBOC) could be determined using with Rcohe/Hitachi 902 ISE Modular Analytics (Mannheim, Germany) without any HBOC separation. Their blood samples, however, had been diluted 8 times in the analyzer. In practice where HBOC would be used for treatment for massive hemorrhage, the HBOC might be contaminated up to 40 % in blood as documented in a guidance for clinical application of the HBOC[16] and thus their corroboration above would not be guaranteed.

Fortunately in this study, we could measure the electrolyte concentrations in the 1/2 mixture with HbV and even in the original HbV with the D method while a few values for K⁺ were exceeded a little beyond the acceptable range. In contrast with the W method the electrolyte concentrations could not be measured while the mixture rate was higher than 1/8 but could be less than 1/16. Reason why definite determination could be most done with the D method but not with the W method until the HbV was diluted less than the 1/16 remained obscure. It also remained to reveal that the liposome vesicle per se or liposome enclosed hemoglobin would affect on measurement with the W method.

In processing the HbV formation, namely encapsulation of hemoglobin solution which obtained from hemolysed red cells, K⁺ should be enclosed into liposome vesicle. The vesicles were rinsed several times with physiological saline after the encapsulation. In fact, Na⁺ in the HbV was found at concentration of 154.5 ± 2.1 mEq/L with the D method and 151.5 ± 0.8 mEq/L with the W method. However K⁺ concentration for the HbV per se and the medium separated was determined as 0.35 ± 0.01 mEq/L and 0.40 ± 0.02 mEq/L with the W method, respectively. Liposome membrane is defined as semipermeable by Chang[17]. Therefore possibility that K⁺ might diffuse out through the liposome membrane during storage could be anticipated. This possibility remained also to be revealed in the future.

Incidentally any abnormal findings were noted on neither hematocrit nor hemoglobin value for the blood donated by volunteers.

5. Summary

It was confirmed that the dry method mounted on Vitros200™ (Orho Clinical Diagnostics) was most adaptable to determine electrolyte concentrations, such as Na^+, K^+, and Cl^-, in serum containing the HbV. On the other hand, the wet method mounted on TBA200FRNEO™ (Toshiba Medical System) was limited to determine them until the HbV would be mixed less than 1/16. Reason for the limited capacity for the wet method remained to be explained in the future. Reason for presence of trace amount of K^+ in the HbV and for possible permeation of ions through liposome membrane also remained to be studied.

6. Acknowledgement

References

1. Takaori M. Artificial oxygen carriers : Looking forward to its future, Artif Blood 2007; 25: 90-98. (in Japanese)
2. Gibson QH. The kinetics of reactions between haemoglobin and gases. In : Butler JAV, Katz B, eds. Progress in Biophysics and Biophysical Chemistry. New York : Pergamon Press, 1959; 1-54.
3. Motterlini R, MacDonald VW. Cell-free hemoglobin potentiates acetylcholine-induced coronary vasoconstriction in rabbit hearts. J Appl Physiol 1993; 75: 2224-2233.
4. Katusic ZS, LeeHC, Clambey ET. Crosslinked hemoglobin inhibits endothelium-dependent relaxations in isolated canine arteries. Eur J Pharmacol 1996; 299: 239-244.
5. Natanson C, Kern SJ, Lurie P, Banks SM, Wolfe SM. Cell-free hemoglobin-base blood substitutes and risk of myocardial infarction and death - A meta-analysis. JAMA 2008; 299: 2304-2312.
6. Callas DD, Clark TL, Moreira PL, Lansden C, Gawry MS, Kahn S, Bermes EWJr. In vitro effects of a novel hemoglobin-based oxygen carrier on routine chemistry, therapeutic drug, coagulation, hematology, and blood bank assays. Clin Chem 1997; 43: 1744-1748.
7. Wolthuis A, Peek D, Scholten R, Moreira P, Gawry M, Clark T, Westrhuis L. Effect of the hemoglobin-based oxygen carrier HBOC-201 on laboratory instrumentation : Cobas integra, Chiron blood gas analyzer 840, Sysmex SE-9000 and BCT. Clin Chem Lab Med 1997; 37: 71-61.
8. Jahr JS, Osgood S, Rothenberg SJ, Li QL, Butch AW, Osggod R, Cheung A, Driessen B. Lactate measurement interference by hemoglobin-base oxygen carriers (Oxyglobin™, Hemopure™, and Hemolink™). Anesth Analg 2005; 100: 431-437.
9. Miyake S, Ohashi Y, Takaori M. Blood type determination for blood which contains hemoglobin based artificial oxygen carrier : Special reference to automated analyzer. Artif Blood 2007; 15: 85-89. (in Japanese)
10. Ali AA, Ali GS, Steinke JM, Shepherd AP. Co-oximetry interference by hemoglobin-based blood substitutes. Anesth Analg 2001; 92: 863-869.
11. Murata M, Komine R. Effects of hemoglobin vesicles on blood cells, blood coagulation and fibrinolysis Report for Japanese Ministry of Health, Welfare and Labor Research Project "Studies on improvement on safety of Artificial Oxygen Carrier H17-Regulatory Science for Medical Drug & Instrument - 074" with Chief Investigator Kobayashi, K. April 2006 : 34-40 (in Japanese)
12. Takaori M, Fukui A. Treatment of massive hemorrhage with liposome encapsulated human hemoglobin (NRC) and hydroxyethyl starch (HES) in beagles. Artif Cells Blood Subst Immob Biotech 1996; 24: 643-653.
13. Murata M. Optimization on laboratory examination for blood specimens contained hemoglobin vesicles (HbV). Artif Blood 2007 ; 15: 22 (in Japanese)
14. Sou K, Komine R, Sakai H, Kobayashi K, Tsuchida E, Murata M. Clinical laboratory test of blood specimens containing hemoglobin vesicles Interference avoidance by addition dextran. Artif Blood 2009; 17: 6-15. (in Japanese)
15. Cameron SJ, Gerhardt G, Engelstad M, Young MA, Norris EJ, Sokoll LJ. Interference in clinical chemistry assays by the hemoglobin-based oxygen carrier, Hemospan™. Clin Biochem 2009; 42: 221-224.
16. Takaori M. Approach to clinical trial considering medical ethics and efficacy for HbV, liposome encapsulated hemoglobin vesicle. Artif Cells Blood Subst Immob Biotech 2005; 33: 65-73.
17. Chang TMS. Semipermeable aqueous microcapsules (artificial cells) with emphasis on experiments in an extracorporeal shunt system. Trans Am Soc Artif Intern Organs 1966; 12: 13-19.

人工酸素運搬体(HbV)を含む血清での電解質測定

三宅誠司，武村次郎(大阪府済生会野江病院検査科)，高折益彦(東宝塚さとう病院)

要約　オーソ・クリニカル・ダイアグノステイック社製ビトロス250™を用いたdry法はリポソーム膜に包埋されたヘモグロビン粒子である人工酸素運搬体（HbV）が共存しても血清中の血清電解質（Na⁺，K⁺，Cl⁺）濃度の測定で臨床的に十分耐えら得るものと評価された．一方，東芝メデイカルシステムズ（TBA200FRNEO™）を使用したwet法での測定ではHbVが1/8までの混入では予想濃度値との間に差を生じた．しかし1/16以下の混入においては臨床検査値として認容される精度で測定可能であった．

wet法において一定濃度以下のHbV混入にならないと上記血清中電解質の濃度測定ができなかった理由，さらにwet法で僅かながら検出されたHbV，およびHbV浮遊液中のK⁺の由来については今後に研究する課題として残された．

Static Structures and Dynamics of Hemoglobin Vesicle (HbV) Developed as a Transfusion Alternative

Takaaki Sato,[†,‡] Hiromi Sakai,[*,‡] Keitaro Sou,[‡] Martin Medebach,[§] Otto Glatter,[§] and Eishun Tsuchida[*,‡]

International Young Researchers Empowerment Center, Shinshu University, Tokida 3-15-1, Ueda 386-8567, Japan, Research Institute for Science and Engineering, Waseda University, Okubo 3-4-1, Shinjuku-ku, Tokyo 169-8555, Japan, and Physical Chemistry, Institute of Chemistry, University of Graz, Graz A-8010, Austria

Hemoglobin vesicle (HbV) is an artificial oxygen carrier that encapsulates solution of purified and highly concentrated (ca. 38 g dL^{-1}) human hemoglobin. Its exceptionally high concentration as a liposomal product (ca. 40% volume fraction) achieves an oxygen-carrying capacity comparable to that of blood. We use small-angle X-ray scattering (SAXS) and dynamic light scattering (DLS) to investigate the hierarchical structures and dynamics of HbVs in concentrated suspensions. SAXS data revealed unilamellar shell structure and internal density profile of the artificial cell membrane for Hb encapsulation. The SAXS intensity of HbV at scattering vector $q > 0.5$ nm^{-1} manifests dissolution states of the encapsulated Hbs in the inner aqueous phase of the vesicle having ca. 240 nm diameter. The peak position as well as the height and width of static structure factor of Hb before and after encapsulation are almost identical, demonstrating the preserved protein—protein interactions in the confined space. To overcome multiple scattering from turbid samples, we employed thin layer-cell DLS combined with the so-called bruteforce and echo techniques, which allows us to observe collective diffusion dynamics of HbVs without dilution. A pronounced slowdown of the HbV diffusion and eventual emergence of dynamically arrested state in the presence of high-concentration plasma substitutes (water-soluble polymers), such as dextran, modified fluid gelatin, and hydroxylethyl starch, can be explained by depletion interaction. A significantly weaker effect of recombinant human serum albumin on HbV flocculation and viscosity enhancement than those induced by other polymers is clearly attributed to the specificity as a protein; its compact structure efficiently reduces the reservoir polymer volume fraction that determines the depth of the attractive potential between HbVs. These phenomena are technically essential for controlling the suspension rheology, which is advantageous for versatile clinical applications.

Introduction

Phospholipid vesicles, often called liposomes, encapsulating or embedding functional drugs, have long been investigated for their practical use as drug-delivery systems. They in part have already been approved for antifungal or anticancer therapy.[1] Hemoglobin vesicle (HbV), or liposome encapsulated Hb, is an artificial oxygen carrier that encapsulates a purified and highly concentrated Hb solution in a phospholipid vesicle.[2–7] The safety and an oxygen-carrying capacity of HbV as a transfusion alternative have been evaluated in animal tests.[7–9] Its exceptionally high concentration ([Hb] = 10 g dL^{-1}; [lipids] = ca. 6 g dL^{-1}, volume fraction, ca. 40%) compared to any other conventional liposomal products for medical use offers sufficient oxygen-carrying capacity comparable to that of blood. HbVs are now widening their uses, aimed at other novel clinical applications, such as the oxygenation of ischemic tissues and the ex vivo perfusion system.[10]

Significant functional consequences of the cellular structure of the red blood cells (RBCs) are the retardation of entrapment of endogenous vasorelaxation factors (NO and CO),[11,12] preservation of chemical environments, such as enzymes for metHb reduction and allosteric effectors, screening of high colloid osmotic pressure (COP) of a concentrated Hb solution, and so forth. By mimicking RBCs, HbV is equipped with the hierarchically organized cellular structures despite its far smaller size.[2,3,7–9] Owing to this notable feature, serious side effects of molecular Hb that exhibits a high COP and causes vasoconstriction due to its specific affinity to NO and CO can be avoided.[13,14] Successful fabrication of the HbV fine particle was previously confirmed by indirect mathematical calculation of lamellarity and intracellular Hb concentration using the particle size and the total concentrations of the components in a dispersion or microscopic observation of a dried sample.[15,16] However, statistically valid, full structural characterization of HbV in a dispersion state remains to be done. In particular, microscopic internal structures of the phospholipid bilayer membrane whose composition is precisely optimized for Hb encapsulation and long-time preservation, and the dissolution state of the concentrated Hbs confined into the inner aqueous phase of the vesicle are of great interest. To access such structural details, we used small-angle X-ray scattering (SAXS).[17,18]

On the one hand, the preservation or adjustment of COP is one of the important requirements for a transfusion alternative

* To whom correspondence should be addressed. E-mail: (H.S.) hiromi@waseda.jp; (E.T.) eishun@waseda.jp. Phone: +81-3-5286-3122. Fax: +81-3-3205-4740.
† Shinshu University.
‡ Waseda University.
§ University of Graz.

to sustain the blood circulation. In the human body, human serum albumin (HSA), the most abundant plasma protein in our bloodstream (dissolved at ca. 5 g dL^{-1}), preserves COP of blood (ca. 20 Torr).[19] Since HbV suspended in saline solution does not contribute to COP of blood, HbV must be coinjected with a solution of HSA or other plasma substitutes (water-soluble polymers) for its clinical use. However, an addition of nonadsorbing polymers to a suspension of colloidal particles generally induces an aggregation tendency of colloidal particles, as known to occur for various particle systems, such as polystyrene beads, silica, liposomes, and RBCs.[20-25] At high enough polymer volume fraction, it often causes phase separation. A theoretical description on this intriguing phenomenon was first given by Asakura and Oosawa;[26,27] exclusion or depletion of small particles or polymer molecules from the region closely spaced large colloid particles lead to an effective attractive potential between the two large particles, increasing the overall disorder.[26-31] This entropic driven force is of fundamental importance as well as technologically implicative, as highlighted by the practical use of nonadsorbing polymers as rheological modifiers for colloidal products. This is indeed valid for medical applications of HbVs; as we have shown, the combination of HbV and different plasma substitute solutions provide an opportunity to manipulate the suspension rheology.[32,33]

From a physiological and medical point of view, high viscosity fluid is often advantageous for increasing blood viscosity to sustain peripheral blood flow because the resulting increase in shear stress on the vascular wall promotes the production of vasorelaxation factors, such as nitric oxide and prostacyclin.[32-36] The HbV suspended in solution of recombinant HSA (rHSA) behave nearly as a Newtonian fluid,[3,32,38] whereas other polymers, such as hydroxylethyl starch (HES), dextran (DEX), and modified fluid gelatin (MFG) medically used worldwide in medical treatments,[39-41] lead to non-Newtonian behavior and hyperviscosity.[32] This is possibly due to HbV flocculation induced by depletion interaction. To gain deeper insights into the underlying mechanism, we used thin layer-cell dynamic light scattering (TC-DLS)[42,43] combined with bruteforce[44] and echo[43-45] techniques. This enables us to observe collective diffusion in a concentrated HbV suspension and its mixtures with plasma substitutes without dilution, overcoming the interference from multiple scattering of turbid samples. The results are not only implicative in interdisciplinary fields of soft-condensed matter physics and biochemistry but are of practical importance for a new class of forthcoming medical applications.

Experimental Section

Materials. The HbV was prepared under sterile conditions, according to the previously reported procedures.[15,46,47] Hbs are purified from outdated donated blood provided by the Japanese Red Cross Society (Tokyo, Japan). The Hb solutions for encapsulation were prepared from this stock solution by adjusting the concentration to 38 g dL^{-1}. The encapsulated purified Hb contained 14.7 mM pyridoxal 5'-phosphate (PLP; Sigma) as an allosteric effector in a molar ratio of PLP/Hb = 2.5. The lipid bilayer membrane for the Hb encapsulation comprises 1,2-dipalmitoyl-sn-glycero-3-phosphatidylcholine, cholesterol, and 1,5-bis-O-hexadecyl-N-succinyl-L-glutamate, mixed in the molar ratio of 5:5:1 (Nippon Fine Chemical Co. Ltd., Osaka, Japan) and 1,2-distearoyl-sn-glycero-3-phosphatidylethanolamine-N-poly(ethylene glycol) (NOF Corp., Tokyo, Japan) at 0.3 mol % of the total lipid. The HbVs were suspended in a

TABLE 1: Plasma Substitute Solutions and Their Physicochemical Properties[a]

plasma substitute	M_w (kDa)	c (g dL^{-1})	COP (Torr)	R_g (nm)
rHSA	67	5.0	19	2.84[b]
HES$_{70}$	68	6.0	34	5.96[b]
HES$_{130}$	130	6.0	35	6.83[b]
HES$_{670}$	670	6.0	27	12.95[b]
DEX	40	10.0	44	4.96[b]
MFG	30	4.0	44	5.50[b]

[a] rHSA, recombinant human serum albumin; DEX, dextran; HES, hydroxyethyl starch; MFG, modified fluid gelatin; COP, colloid osmotic pressure. [b] R_g for plasma substitutes except rHSA was obtained with Guinier plot of SAXS data obtained at $c = 1$ g dL^{-1}, and that for rHSA was calculated by using Guinier plot[17] against the form factor $P(q)$ obtained as an output of GIFT[52-54] procedure for $c = 1$ g dL^{-1}.

physiologic saline solution at [Hb] = 10 g dL^{-1} ([lipids] = ca. 6 g dL^{-1}) and were deoxygenated for storage with N_2 bubbling in vials.[48]

The plasma substitutes used in this study are listed in Table 1. rHSA ($M_w = 67$ kDa, 25 g dL^{-1}) was a gift from Nipro Corp. (Osaka, Japan). A DEX solution ($M_w = 40$ kDa, 10 g dL^{-1} in a physiological saline solution) was purchased from Kobayashi Pharmaceutical Co. Ltd. (Osaka, Japan). Solutions of HES with different molecular weights were assorted; an HES$_{70}$ solution (Saline-HES, $M_w = 68$ kDa, 6 g dL^{-1} in a physiological saline solution) was purchased from Kyorin Pharmaceutical Co. Ltd. (Osaka, Japan). An HES$_{130}$ solution (Voluven, $M_w = 130$ kDa, 6 g dL^{-1} in a physiological saline solution) was a gift from Fresenius Kabi AG (Homburg v.d.H., Germany). An HES$_{670}$ solution (Hextend, $M_w = 670$ kDa, 6 g dL^{-1} in a physiological Ringer lactate solution) was obtained from Hospira, Inc. (Lake Forest, IL). An MFG solution (Gelofusin, $M_w = 30$ kDa, 4 g dL^{-1} in a physiological saline solution) was a gift from B. Braun Melsungen AG (Melsungen, Germany). As a standard for testing the accuracy of our dynamic light scattering (DLS) experiments, a pseudomonodisperse microsphere with a nominal diameter of 0.209 μm with a 0.011 μm standard deviation (Polyscences, Inc., U.S.A.) was used.

For optimized experimental conditions, the concentration of the HbV dispersions was further adjusted for SAXS and DLS experiments by adding a saline solution (Otsuka Pharmaceutical Co. Ltd., Osaka, Japan) or solutions of plasma substitute, and these samples were immediately used for experiments.

SAXS. We performed SAXS measurements on HbV suspensions and their model systems to examine their static structures. We used a SAXSess camera (Anton-Paar, Graz, Austria) attached to a PW3830 sealed-tube anode X-ray generator (PANalytical, Netherlands). The generator was operated at 40 kV and 50 mA. A Göbel mirror and a block collimator provide a focused monochromatic X-ray beam of Cu Kα radiation ($\lambda = 0.1542$ nm) with a well-defined shape. A thermostatted sample holder unit (TCS 120, Anton Paar) was used to control the sample temperature. The 2D scattering patterns recorded by an imaging-plate (IP) detector (a Cyclone, Perkin-Elmer, U.S.A.) were integrated into to one-dimensional scattered intensities $I(q)$ as a function of the magnitude of the scattering vector $q = (4\pi/\lambda)\sin(\theta/2)$ using SAXSQuant software (Anton Paar), where θ is the total scattering angle. For all experiments, we monitored attenuated primary beam at $q = 0$ using a semitransparent beam stop. All the measured intensities were semiautomatically calibrated for transmission by normalizing a zero-q primary intensity to unity. The background scattering contributions from capillary and solvent were corrected. The

absolute intensity calibration was made by using water intensity as a secondary standard.[49]

DLS. We used DLS to study the size and size distribution using a laboratory-built goniometer, equipped with single-mode fiber optics and an ALV single-photon detector (ALV-Laser Vertriebsgesellschaft, Langen, Germany) for detection of a time-dependent scattered intensity. A 8 mm cylindrical sample cell was immersed in a temperature-controlled index match bath filled with decalin solvent. The light source was a Verdi V5 diode laser from Coherent with a wavelength of 532 nm with a maximum output of 5 W. The data acquisition was performed with an ALV 5000 multiple τ-digital correlator. The ALV-5000/E software package was used to calculate the intensity time-correlation functions.

TC-DLS. In order to overcome the problems of multiple scattering from turbid samples caused by typically submicrometer particle size and their high concentration, we used a modified TC-DLS technique.[42,43] The TC-DLS apparatus was constructed based on an apparatus originally designed for static light scattering on turbid colloidal dispersions,[50,51] which was equipped with a flat cell with variable thickness of 15, 50, and 100 μm, a single-mode fiber, and the ALV-5000 correlator (ALV-Laser GmbH, Langen Germany) for autocorrelation measurements of the time-dependent scattered light intensity via the fiber and the photomultiplier. A 10mW HeNe laser with a wavelength of 632.8 nm was used as a light source. The current setting allows the measurements of the scattered light between 15 and 45°.

Bruteforce and Echo DLS Experiments for Arrested Media. We used brute-force ensemble averaging technique[44] in combination with echo DLS[43–45] in the TC configuration to achieve a multispeckle observation. The method allows us to pursuit arrested slow dynamics of the HbV particles in flocculation in the presence of a kind of plasma substitute. Under the condition that an ergodicity assumption is violated, that is, when equivalence of time-averaging with ensemble-averaging is not fulfilled, conventional DLS approaches based on a time-averaging of the intensity fluctuations of a single speckle become no longer valid. In order to achieve a proper ensemble averaging, we used for short time correlation times the brute-force ensemble averaging in which we monitored intensity fluctuations from many independent speckles, performing repeated short-time measurements for several hundreds of different sample cell configurations. For the measurements of the long-time tail of intensity correlation functions in the correlation time range of $\tau >$ 10 s, we used echo technique; if the intensity correlation function is measured with the sample cell precisely rotated, it allows the exploration of many independent sample configurations during one evolution of the rotation, avoiding a significantly longer time-averaging. In such an experiment, the ensemble averaged correlation function can be measured with relatively short averaging time. The echo peaks appear at multiples of $1/f$, where f is the frequency of the rotation, and the peak height slowly decays, reflecting the slow dynamics of the particles.

Results and Discussions

Particle Characterization of HbV in a Dilute Dispersion. The intensity autocorrelation function, $g_2(t)$, measured in the homodyne mode is connected to the normalized field correlation function, or the dynamic structure factor, $g_1(t)$, via the relation

$$g_2(t) = 1 + \beta |g_1(t)|^2 \qquad (1)$$

where β is called coherence factor. The present experimental setup using single-mode fiber detection attains nearly its
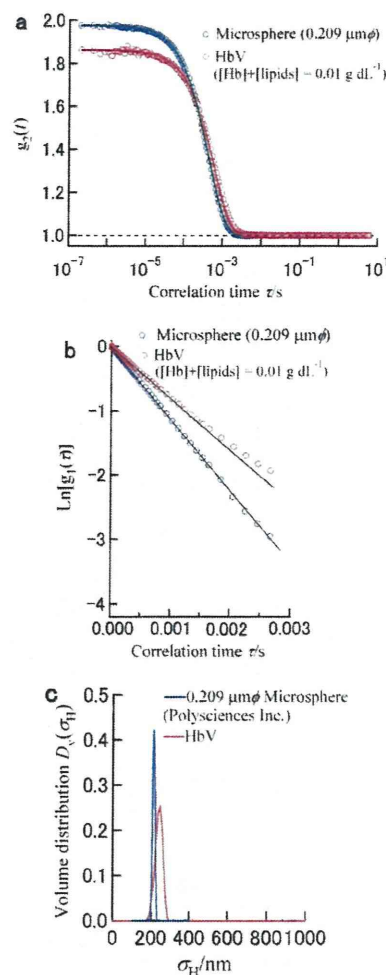

Figure 1. The particle characterization of HbV in a dilute dispersion as obtained by DLS. Intensity correlation functions, $g_2(t)$, of a dilute HbV dispersion ([Hb] = 6.3×10^{-3} g dL^{-1}) and a 0.027 wt % dispersion of pseudomonodisperse microsphere with a nominal averaged diameter of 0.209 μm measured at 25 °C (a), the cumulant fit to the same DLS data (b), and the particle size distribution of the HbV and the microsphere (c), obtained by using ORT.[56]

theoretical maximum of $\beta \sim 1$. In Figure 1, we present particle characterization of the HbV in a dilute dispersion ([Hb] + [Lipids] = 0.01 g dL^{-1}) as obtained by DLS. The effects of structure factor, $S(q)$, as well as hydrodynamic function, $H(q)$, are expected to be negligible at such low concentration. As a control, we tested pseudomonodisperse microsphere with a nominal diameter of 0.209 μm (Polysciences, Inc., U.S.A.) to check the accuracy and the experimental broadening of our DLS experiments. Monodisperse spherical particles exhibits a single-exponential decay of $g_1(t)$

$$g_1(t) = \exp(-Dq^2 t) \qquad (2)$$

where the D is the diffusion constant. D can be related to the hydrodynamic radius R_H of the hardsphere via the Stokes–Einstein relation

$$D = \frac{k_B T}{6\pi \eta R_H} \qquad (3)$$

where k_B is Boltzmann constant, T is temperature, and η is solvent viscosity. The intensity correlation functions, $g_2(t)$, of

Static Structures and Dynamics of HbV

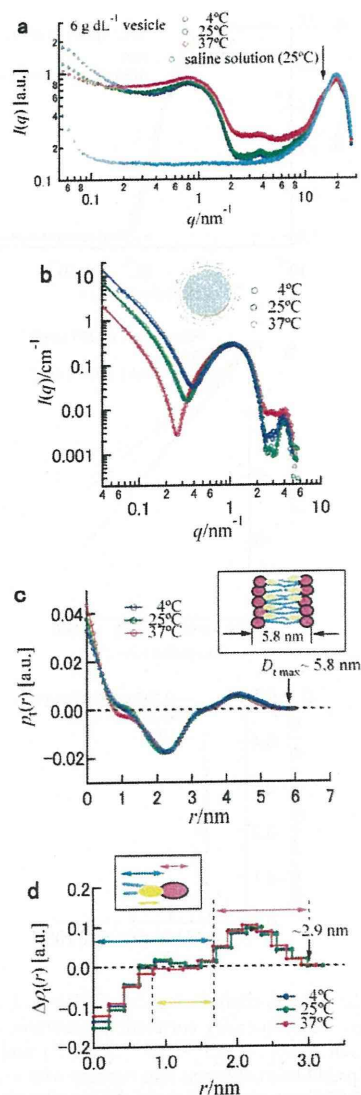*J. Phys. Chem. B, Vol. 113, No. 24, 2009* **8421**

Figure 2. Structural characterization of a phospholipid bilayer membrane for Hb encapsulation as obtained by SAXS. Small and wide-angle X-ray scattering (SWAXS) intensity in $0.05 \leq q/\text{nm}^{-1} \leq 27$ (a), collimation-corrected SAXS intensities on absolute scale (b), the thickness pair-distance distribution function, $p_t(r)$ (c), and electron density profile deconvoluted from $p_t(r)$ (d) of a 6 g dL^{-1} dispersion of the vesicle for Hb encapsulation as a function of temperature. In the insets of panel c and d, the structure of the lipid bilayer is schematically shown. A light blue line and a pink ellipse respectively represent hydrophobic chain and hydrophilic headgroup of the lipids, and a yellow ellipse stands for cholesterol.

both diluted dispersions of the HbV and the microsphere exhibit single-step relaxation behavior and a rapid convergence to the baseline (unity). For particle systems having a rather narrow size distribution that typically show single-step relaxation behavior, the second-order cumulant analysis[55] is often employed. The technique can be used as a convenient and fast method for obtaining a semiquantitative measure of the mean size and the width of its distribution. In Figure 2b, we display the cumulant plot, namely, a natural logarithm of the field correlation function, $\ln[g_1(t)]$, of the same DLS data shown in Figure 2a. Despite a smaller intercept for the HbV ($\beta \sim 0.85$), which is probably due to absorption of the hemoprotein, the slower decay of $g_1(t)$ for the HbV reflecting larger averaged size is apparent in this plot. The $g_1(t)$ of the microsphere shows almost ideal linear behavior up to its long-time tail, indicating

a quite narrow relaxation time distribution, whereas that of HbV represents still small but clear deviation from the straight line at large τ, implying wider relaxation time distribution due to its size distribution. The cumulant analysis yielded $R_H = 143$ nm and 34.8% width of size distribution for HbV, and $R_H = 107$ nm and 6.6% width for the pseudomonodisperse microsphere.

For further quantitative discussion, we also carried out a more detailed mathematical analysis. We evaluated the size-distributions by using optimized regularization technique (ORT),[56] which relies on (indirect) inverse Laplace transformation of the experimental field correlation function, $g_1(t)$, into the relaxation-rate distribution functions. Assuming a linear combination of single exponential functions, $g_1(t)$ of polydisperse systems may be given by

$$g_1(t) = \int_{\Gamma_{\min}}^{\Gamma_{\max}} G(\Gamma)\exp(-\Gamma t)\mathrm{d}\Gamma \qquad (4)$$

The exponent Γ is proportional to the diffusion constant D as $\Gamma = Dq^2$. For the actual ORT evaluation, eq 4 is replaced with

$$g_1(t) = \int_{\tau_{\min}}^{\tau_{\max}} D(\tau)W(\tau)\exp(-t/\tau)/\tau^2 \, \mathrm{d}\tau \qquad (5)$$

where $D(\tau)$ is the distribution function, $W(\tau)$ is the weighting function, and $\Gamma = 1/\tau$. $W(\tau) = 1$ gives intensity distribution, and for volume or mass distribution, $W(\tau) = \tau^3$. We present the deduced volume distribution function of hydrodynamic diameter $D_V(\sigma_H)$, where $\sigma_H = 2R_H$. The ORT analysis provided a spikelike size distribution for the microsphere, which confirms negligibly small experimental broadening of our DLS experiments for the present purpose. The analysis on the HbV dispersion yielded an averaged hydrodynamic diameter, σ_H, of 238 nm and a narrow size distribution with a 20 nm standard deviation in the volume distribution. The data demonstrate well-controlled geometry of the HbV particles as molecular assembly.

Structural Characterization of the Phospholipid Bilayer Membrane for Hb Encapsulation. Figure 2 shows the X-ray scattered intensities $I(q)$ for a 6 g dL^{-1} dispersion of the vesicles without Hb encapsulation at different temperatures, prepared as a counterpart model system of HbV. The raw SWAXS data as obtained, shown in Figure 2a, confirm the absence of the so-called α-gel peak at $q \sim 15$ nm^{-1}, corresponding to interchain spacing of $d = 0.42$ nm, at all investigated temperatures. Although the α-gel–liquid crystalline phase transition temperature of DPPC is known to be 41 °C, this confirms a melted state of the hydrophobic chains in the lipid bilayers and high lateral fluidity of lipids even at 4 °C owing to the presence of cholesterol.

The (collimation corrected) absolute intensities after the background subtraction, $I(q)$, are displayed in Figure 2b as a function of temperature. As is well-known, multilamellar stacks give equidistant peaks due to their structure factor. However, the low-q part ($q < 0.3$ nm^{-1}) of $I(q)$ exhibits neither an interbilayer interference peak nor its faint signature like an undulation. This finding indicates that as we designed, the structure of vesicle is, at least for the most part, unilamellar.

The quantitative analysis of the bilayer thickness and internal density fluctuation is possible, while the maximum diameter of the vesicle (ca. 240 nm) by far exceeds the maximum resolution of our SAXS experiments. The theoretical descriptions of scattering functions from a multilamellar stack of bilayers can be summarized as follows.[57] Assuming monodisperse bilayers,